FINAL REPORT

Characterization of Advanced Electronic and Optoelectronic Semiconducting Materials Using Synchrotron Radiation Diffraction Imaging for Control of Crystal Growth and Fabrication

(Contract # 70NANB8H0810)

Submitted to: Dr. Masao Kuriyama
US Department of Commerce - NIST
Ceramics Division Room A163
Gaithersburg, MD 20899

Submitted by: Stuart R. Stock
School of Materials Engineering
Georgia Institute of Technology
Atlanta, Georgia 30332-0245

February 12, 1990

Program Objectives

The objectives of this program were:

1. To exploit recent advances in synchrotron radiation imaging for detailed characterization of defects in high quality III-V and II-VI crystals,
2. To perform detailed characterization of grain boundaries and other crystallographic defects in mercuric iodide,
3. To correlate specific device performance difficulties with observed growth and processing defects and
4. To use the knowledge gained to improve crystal growth, processing and device performance.

Development of this fundamental knowledge was to assist U.S. industrial/technological competiveness in the area of microelectronics.

Program Accomplishments

The program was originally intended to span two years, but priorities at the funding agency dictated that the project be funded for only one year. Additional funding for three months for a related task and a no-cost extension made the program duration 4/1/88 - 9/30/89. The impact of these changes dictates that the program's accomplishments are somewhat different from those listed above.

Participation in imaging experiments of Dr. Kuriyama's group was more limited than originally intended. Dr. Gartstein made three trips to NSLS and Dr. Stock made one trip. In part this was due to relatively long stretches without beamtime and in part due to the unanticipated unavailability of Dr. Stock due to personal reasons. Dr. Gartstein's participation was also limited since it was decided early on that he could make a more significant contribution on the theoretical rather than the experimental side.

Considerable sample characterization was undertaken, however, in preparation for the trips of others to NSLS. The characterization work was precise orientation of samples with the back-reflection Laue technique. Considerable effort was devoted to computer simulation programs for interpreting complex x-ray topographic images. A paper based on this work has been submitted for publication by Dr. Gartstein and is entitled "Multiple-Beam Calculation of the Intensity Distribution for an Imperfect Crystal in Laue Geometry." A copy of this manuscript is attached as an Appendix.

Dr. Gartstein also wrote a report for Dr. L. Schwartz which covered the options for diffraction imaging of materials using synchrotron radiation. Of particular interest was the use of microdiffraction from small crystals or from single grains in polycrystalline metals and ceramics.

The one trip to NSLS for Dr. Stock to collaborate with Dr. Kuriyama's group was very successful. Use of the monochromatic radiation for imaging break-down regions in In-alloyed GaAs produced some very interesting results on a crystal from Hewlett-Packard. Videotape images of diffracted intensity as a function of sample orientation revealed the origin of blank regions previously seen in white beam topographs of the same crystal: these relatively small volumes diffract at a significantly different angle. This is persuasive, but not conclusive evidence, that these cells (and perhaps others) are bounded by subgrain walls. If the angles are small and if the misorientation axes are randomly oriented, it is not surprising that only a few cells will be out of contrast for a given set of diffraction planes and sample orientation. Dr. Stock also made an important contribution to the analysis of a GaAs crystal obtained by Dr. Kuriyama's group: he correctly identified the presence of twins in one of their samples from surface features and from the diffraction contrast.

Recommendations

The author was very impressed by the NIST diffraction imaging activity headed by Dr. Kuriyama. This group is by far the most advanced in monochromatic diffraction imaging in the U.S. and is on par with any in the world. The European Community and Japan are currently supporting efforts far in excess of those supported in the U.S., and it is important to our industrial competiveness to maintain parity in this technologically important branch of x-ray diffraction. The role of the NIST diffraction imaging group certainly fits the mission of NIST. Therefore, the author urges that the strongest possible support be given Dr. Kuriyama's group. This recommendation holds regardless of whether the Georgia Tech group continues to collaborate with Dr. Kuriyama's group.

Efim Gartstein

MULTIBEAM CALCULATION of the INTENSITY DISTRIBUTION for an IMPERFECT CRYSTAL in LAUE GEOMETRY.

National Institute of Science and Technology, Ceramics Division, Gaithersburg MD 20899

A scattering matrix formalism of the multibeam dynamical X-ray theory is applied to calculate the intensity distribution for an imperfect crystal in Laue geometry. The computational procedure for the solution of this problem is presented. Simulation performed for a particular imperfect structure suggests that this method can be useful for detailed structure modelling.

1. Introduction.

Depending on the degree of imperfection of the crystals the kinematical or dynamical X-ray theories have to be employed to determine their structure. In the kinematical theory the single scattering process of an X-ray photon is justified as long as the coherent regions are very small, such as in the mosaic crystals. On the other extreme, perfect crystals representing a single coherent region where multiple scattering occurs the dynamical theory based on two-wave approximation provides an adequate solution to the diffraction problem. Then there is a wide range of imperfect materials, espessially the ones used in the semiconductor industry, with spatially coherent regions large enough for a multiple scattering to occur. It was suggested by Kuriyama [1] that a multibeam dynamical theory should be used to treat such materials. This follows from the fact that for an imperfect crystals the

reflection in reciprocal space will no longer be a point but will have a certain shape depending on the intrinsic structure. In this case the Ewald sphere will have numerous intersections with the reflection and the corresponding number of the beams will be excited in the crystal.

In electron diffraction where the multiple scattering effects are strong the multi-beam dynamical theory was given an extensive treatment [2,3]. For the Laue-case electron diffraction Fujimoto [4] developed scattering matrix formalism. Kuriyama [5] introduced the concept of scattering matrix for the Laue-case in X-ray diffraction. The solution of the multibeam dynamical theory requires numerical computations and this will be discussed in section 2.

In many instances the derivation of the structure by using Fourier transform techniques can not be done as the phase of the scattering amplitudes is not easily obtainable. Another method would be to compare the measured intensity patterns with the simulated ones based on various model structures. The commonly used simulation procedure is the calculation of the rocking curves by solving Takagi-Taupin equations in two beam approximation [6,7,8]. But as it was mentioned above the correct dynamical theory has to consider multibeam interaction of the X-ray photon inside the crystal. An example of such simulation will be given in section 3.

The reported in the literature calculations of the multibeam X-rays diffraction were mostly limited to the cases of simultaneous fundamental reflections in perfect crystal. The purpose of this paper is to demonstrate the applicability of the multi-beam dynamical theory for the treatment of imperfect crystals.

3. Theory and computational procedure.

Here we shall consider the beam incident on the plane-parallel crystal to be a monochromatic plane wave linearly polarized perpendicular to the scattering plane. Such condition can be achieved with a collimated synchrotron radiation by using an asymmetric

diffraction from a monochromator crystal. We shall assume that a total of N waves are excited inside the crystal corresponding to the number of the reciprocal lattice points lying on the Ewald sphere. This scattering geometry is shown in Fig. 1. The 'O'-point designates the ray in the direction of the incident beam and the 'H'-point is in the direction of the ray scattered at $2\Theta_B$ angle. M_O is the number of rays which are due to the intersection of the O-reflection with the Ewald sphere and M_H is the corresponding number due to the H-reflection. The multiple scattering of the X-ray photon in the crystal will produce energy flow in different directions inside the crystal. Another M_{OH} points lying on the Ewald sphere were chosen between 'O' and 'H'-points to account for this effect.

The incident ray 'O' in the crystal defines the origin of the reciprocal space and the wavevectors of the excited waves are related by:

$$\bar{K}_i = \bar{K}_O + \bar{H}_i \quad , \qquad (1)$$

where i is the index of the rays in the crystal corresponding to the reciprocal lattice vector $\bar{H}_i$ as it is shown in the Fig. 1. We shall assume that with a detector of an ideal resolution we can measure the intensity of any ray i deviating from 'O' or 'H'-directions by an angle φ_i. The angular settings of the detector and crystal define the reciprocal lattice vectors $\bar{H}_i$.

The total wavefield in the crystal can be expressed as a superposition of the excited plane waves. This wavefield is described by the fundamental set of equations in the dynamical theory [9] as:

$$\frac{K_i^2 - k^2}{k^2} \bar{E}_i - \sum_j \chi_{i-j} \bar{E}_j = 0 \qquad (2)$$

where $k = 2\pi/\lambda$, λ is the wavelength of X-rays in the vacuum, $\bar{K}_i$ is the wavevector associated with the H_i reciprocal lattice point, $\bar{E}_j$ is the electric field amplitude and is

associated with the same reciprocal lattice point and χ_{i-j} is the Fourier component of the polarizability per init volume for the reflection H_{j-j} . For N excited waves there are N equations for the amplitudes $\bar{E}j$. This can be written in a matrix form as:

$$WE=0 \qquad (3).$$

The simultaneous solution for the amplitudes $\bar{E}j$ will be nontrivial only if the determinant

$$|W|=0 \qquad (4)$$

The relation (4) describes the dispersion surface which is the origin of the wavevectors in the reciprocal space as a function of the angular orientation of the crystal. Due to the boundary conditions of the continuity of the tangential components of the wavevectors at the entrance surface the relations between $\bar{K}_i$ and $\bar{k}$ are:

$$\bar{K}_0=\bar{k}-kq\bar{n} \qquad \text{and} \qquad \bar{K}_i=\bar{k}+\bar{H}_i-kq\bar{n} \qquad (5)$$

where $\bar{n}$ is the unit vector normal to the crystal surface and inwardly directed, q determines the distance between the origin points of the vectors $\bar{k}$ and $\bar{K}_0$. Introduction of the first order approximation that $|K_0|=|\bar{k}|$ allows to linearize the set of equations (3) by replacing:

$$\frac{K_i^2-k^2}{k^2}=\chi_0-2q\gamma_i+2\cdot(-1)^p\Delta\theta\sin 2\theta_B \qquad (6)$$

where $\gamma_0=\bar{k}_B\bar{n}/k$, $\bar{k}_B$ is the wavevector of the incident wave exactly fullfilling the Bragg condition, $\gamma_i=(\bar{k}_B+\bar{H}_i)\cdot\bar{n}/k$. The third term in the right hand side of Eq.(6) relates the position of the tie point of the excited wave with wavevector $\bar{K}_i$ on the dispersion surface to the angular deviation $\Delta\theta$ of the incident beam $\bar{k}_0$ from the Bragg angle. Parameter p can be even or odd depending on the following conditions: if $|\bar{k}_0+\bar{H}_i|<|\bar{k}_0|$ then p

is odd when $\Delta\theta > 0$; if $|\bar{k}_0+\bar{H}_i| > |\bar{k}_0|$ then p is odd when $\Delta\theta < 0$. The vector equation (2) can be written as a scalar equation because the field amplitudes $\bar{E}_j$ are normal to the excited wavevectors lying in the scattering plane. It is convinient to redefine the field amplitudes as:

$$A_j = \sqrt{\gamma_j} E_j \qquad (7).$$

After substitution of the Eqs.(6),(7) into Eq.(3) it can be rewritten as:

$$MA = qA \quad , \qquad (8)$$

where the elements of the matrix M are:

$$M_{ij} = -\frac{1}{2}\frac{1}{\sqrt{\gamma_i \gamma_j}}\left(\chi_{i-j} - \alpha_i \delta_{ij}\right) \qquad (9)$$

δ_{ij} is the Kronecker delta function and $\alpha_i = 2\cdot(-1)^p \Delta\theta \sin 2\theta_B$. The relation (8) represents an eigenvalue-eigenvector problem. M is a general complex matrix for a non-symmetric structure with a non-neglegible absorbtion. Thus the eigenvalues and the eigenvectors are also comlex. The eigenvalues q determine the modes of the wavefields in crystal. The real part $(q_n)_r$ is related to the phase and the imaginary part is related to the absorption of n-th wavefield. We shall note here that in the process of linearization half of the modes are removed from the original problem. This is justified because they would correspond to waves of negligible intensity. But this is not the case for a very asymmetrical scattering geometry when the incident or diffracted beam makes an angle less than 1^o–2^o with the corresponding surface [9]. The normalized eigenvector $\bar{A}^n$ has components $A^n_{H_1}, \ldots A^n_{H_i}, \ldots A^n_{H_N}$. The amplitude of the H_j-wave belonging to the n-th wavefield is then $u^n_{H_j} = p_n A^n_{H_j}$,where p_n is some proportionality

coefficient. Using relation (5) the wavefunction for the H_j-reflection can be written as:

$$\psi_{Hj} = \sum_{n=1}^{N} U_{Hj}^{n} \exp(iq_n t)(\exp(i\bar{k}_{Hj} \cdot \bar{r}) \quad , \qquad (10)$$

where t is the thickness of the crystal and $\bar{k}_{Hj}$ is the wavevector of the H_j-reflection in the vacuum. Fujimoto [4] showed how to determine the coefficient β_n by using the boundary condition at the entrance surface for the Laue-case and the orthonormalization property of the eigenvectors. Using his result the wavefunction for the H_j-reflection on the exit surface given in Eq.(10) can be written as:

$$\psi_{Hj} = \sqrt{\frac{\gamma_0}{\gamma_j}} [\exp(itM)_{jO} \cdot \exp(i\bar{k}_{Hj} \bar{r})] \qquad (11)$$

The scattering matrix is given by:

$$S = \exp(itM) \qquad (12)$$

The subscript jO in Eq.(12) corresponds to the element of the scattering matrix in the j-th row and O-th column where O is the number identifying the incident ray in the crystal. As follows from Eq.(11) this matrix element represents the amplitude of the H_j-reflection wave in the crystal. Kuriyama [5] suggested that the calculation of the scattering matrix S can be done by performing spectral decomposition of the matrix M, as:

$$M = D\tilde{M}D^{-1} \quad , \qquad (13)$$

where $\tilde{M}$ is the diagonalized matrix whose elements $\tilde{M}_{jj}$ are the eigenvalues, D is the orthogonal transformation matrix whose elements are the eigenvectors and D^{-1} is the inverse

matrix. The eigenvalue–eigenvector decomposition of a general complex matrix can be performed by a QR–decomposition procedure [10]. Use of the relation (14) results in an amplitude for the H_j–reflection given as:

$$\bar{E}_H = \left[\frac{\gamma_0}{\gamma_H}\sum_{n=1}^{N} D_{Hn} D_{n0} \cdot \exp(i t \tilde{M}_{nn})\right]\bar{E}_0 \qquad (14)$$

where $\bar{E}_0$ is the amplitude of the incident beam in the vacuum. The reflectivity of the difracted beam is calculated as:

$$R_H = \frac{|\bar{E}_H|^2}{|\bar{E}_0|^2} \cdot \frac{\gamma_H}{\gamma_0} \qquad (15)$$

3. Discussion and conclusions.

To perform the calculation according to the procedure outlined above one has to relate the polarizability term χ_{j-j} in Eq.(9) to the structure of the crystal. It is not simple to describe the structure or polarizability for a general case of an imperfect crystal. The treatment of this problem has been discussed by Kuriyama [11]. Here we shall consider GaAs crystal which is assumed to have a domain structure with the antiphase domain boundaries (APB) perpendicular to ‹100› directions. Such structure was discussed by Holt [12] and experimentally observed by Cho et al [13]. When APB is on {100} planes all the bonds across the interface can be only of one type, i.e. Ga–Ga or As–As. The shift vector at the boundary is $\bar{R}=\frac{a}{4}$‹111› where a is the parameter of the unit cell. We shall conceive the structure to be made up of two subcells or domains with the size $D_i a$ and $(M_i - D_i)a$ along the ‹100› direction. Here $M_i a$ is the period of modulation which describes the size of the supercell. The total structure factor is the product of the structure factor of the unit cell with the Laue modulation function. For one dimensional case the Laue function for an H(hkl)–reflection is given as:

$$\frac{1}{M_i}\{\exp[i\pi(D_i-1)h]\frac{\sin(\pi D_i h)}{\sin(\pi h)} + \exp[i\pi(M_i-D_i-1)h]\frac{\sin[\pi(M_i-D_i-1)h]}{\sin(\pi h)}\exp[2\pi i\cdot\vec{H}\cdot\vec{R}] \qquad (16)$$

For a non-symmetric absorbing crystal the comlex structure factor F_H is not equal to $F_{\bar{H}}$. But any of the atomic species can be chosen as the origin of the unit cell because only relative phase information is important. For a reflection with h+k+l =4n in zinc-blende structure the phase factor in expression (16) is the same for any shift vector $\vec{R}$. The simulation was performed for a symmetric (022) reflection for a crystal with a surface normal [100], thickness t=0.05cm and with $M_i=2\cdot10^3$a and $D_i=1\cdot10^3$a. The total number of 198 waves were chosen for this calculation. Around each of the 'O' and 'H'-beams 69 positions were chosen for the detector with an angular step of 30 arcsec. Another 60 positions were taken between 'O' and 'H" beams. The intensity distribution as a function of the sample offset angle $\Delta\theta$ and detector offset angle φ is shown in Fig.2a and Fig.3a around 'H' and 'O' beams, respectively. In the assumed model there is no lattice mismatch across APB or the strain associated with it. So only satellites from the modulated structure can be expected. The intensity modulation can be seen in Fig.2a. The rocking curves for the 'H'- beam calculated with an angular step of 0.5 arcsec. and 5 arcsec. are shown in Fig.2b and Fig.2c, respectively. These rocking curves look different. The fine structure of the peak with the first order satellites observed in Fig.2b are not present in Fig.2c where the main peak is broadened and higher order satellites appear in the pattern. The simulation can be done with any desired resolution but the comparison with the experimental data will require convolution with the instrumental resolution function. The intensity modulation is even more pronounced around 'O' beam as can be seen in Fig.3a and fig.3b. This can explain why the section topographs obtained from the directly scattered 'O' beam show better contrast then the ones obtained in 'H' beam diffraction.

In this example the polarizability was expressed in terms of Fourier series. The same approach can be extended to more complicated structures. De Fountain [14] showed how to express the modulation functions for the scattering power and for the positional parameters by a Fourier series. He also considered a quasi periodic modulated structure. Thus the described approach for multibeam dynamical calculations can be extended to various imperfect structures. These simulations can be performed in a reasonable amount of time with modern computers. The intensity distribution patterns around the directly scattered 'O'-beam and Bragg diffracted 'H'-beam are produced simultaneously and they can be compared for example with the intensity distributions mapped in a high resolution triple-crystal X-ray difractometer [15].

References.

[1] M. Kuriyama, Acta Cryst. A25, 56 (1969).

[2] J. M. Cowley and A. F. Moodie, Acta Cryst. 10, 609 (1957).

[3] A. R. Moon, Z. Naturforsch. 27a, 390 (1971).

[4] F. Fujimoto, J. Phys. Soc. Japan 14, 1558.

[5] M. Kuriyama, Acta Cryst. A31, 774 (1975).

[6] S. Takagi, Acta Cryst. 15, 1311 (1962).

[7] S. Takagi, J. Phys. Soc. Japan 26, 1239 (1969).

[8] D. Taupin, Bull. Soc. Franc. Mineral. Crist. 87, 469 (1964).

[9] Shih-Lin Chang, Multiple Diffraction of X-rays in Crystals, Springer-Verlag (1984)

[10] J. H. Wilkinson and C. Reinsch, Linear Algebra, vol. 2 of Handbook for Automatic Computation, New-York: Springer-Verlag.

[11] M. Kuriyama, J. Phys. Soc. Japan 23, 1369 (1967).

[12] D. B. Holt, J. Phys. Chem. Solids 30, 1297 (1969).

[13] N. H. Cho, B. C. De Cooman, C. B. Carter, R. Fletcher and D. K. Wagner, Appl. Phys. Lett. 47(8), 879 (1985)

[14] D. de Fontain, Local Atomic Arrangements Studied by X-ray Diffraction. Metallurgical Society Conferences, Vol. 36 Eds. J. B. Cohen and J. E. Hilliard. pp. 51-94. New-York: Gordon and Breach (1966).

[15] E. L. Gartstein, J. Appl. Cryst. to be published (1989).

Figure Captions.

1. The multibeam scattering geometry employed in the model.

2a. The intensity distribution around 'H'-beam as a function of sample and detector offset angles for the symmetric (022) Laue reflection. The intensity scale is in arbitrary units and the angles are in arcseconds.

2b. The rocking curve for the "H'-reflection calculated with an angular step of 0.5 arcsec.

2c. The rocking curve for the "H'-reflection calculated with an angular step of 5 arcsec.

3a. The intensity distribution around 'O'-beam as a function of sample and detector offset angles for the symmetric (022) Laue reflection. The,intensity scale is in arbitrary units and the angles are in arcseconds.

3b. The rocking curve for the "O'-reflection calculated with an angular step of 5 arcsec.

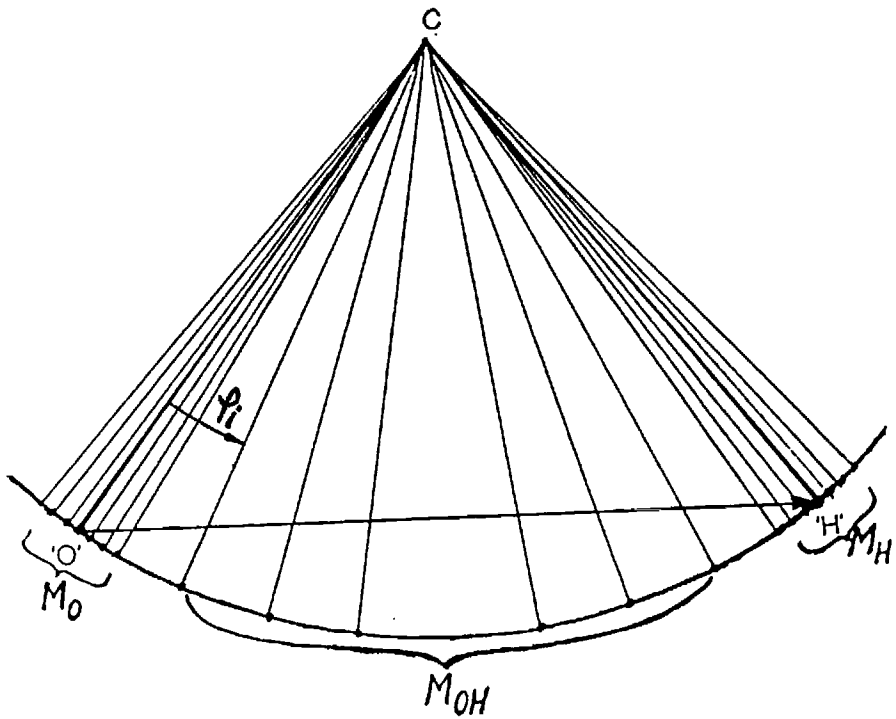

Fig.1

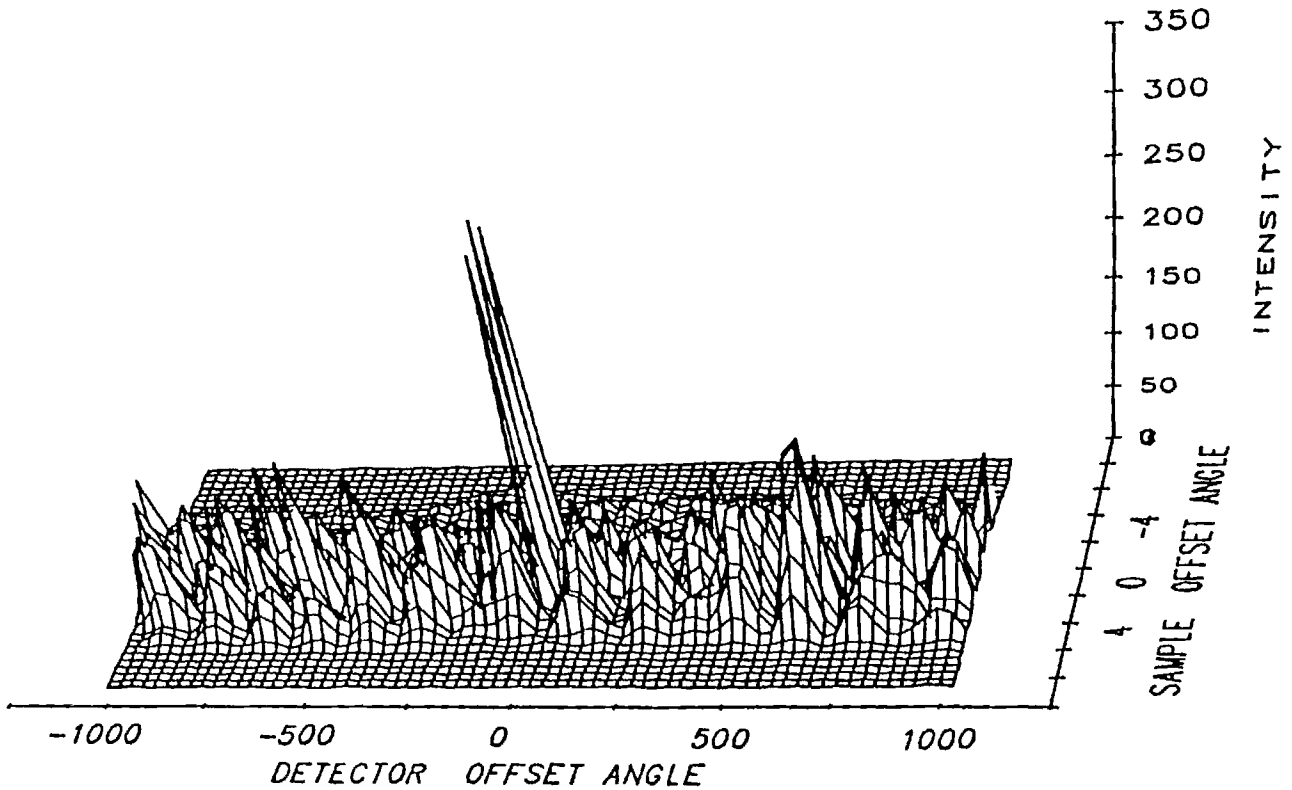
350
300
250
200
150
100
50
0
INTENSITY
4
0
-4
SAMPLE OFFSET ANGLE
-1000
-500
0
500
1000
DETECTOR OFFSET ANGLE

Fig. 2a

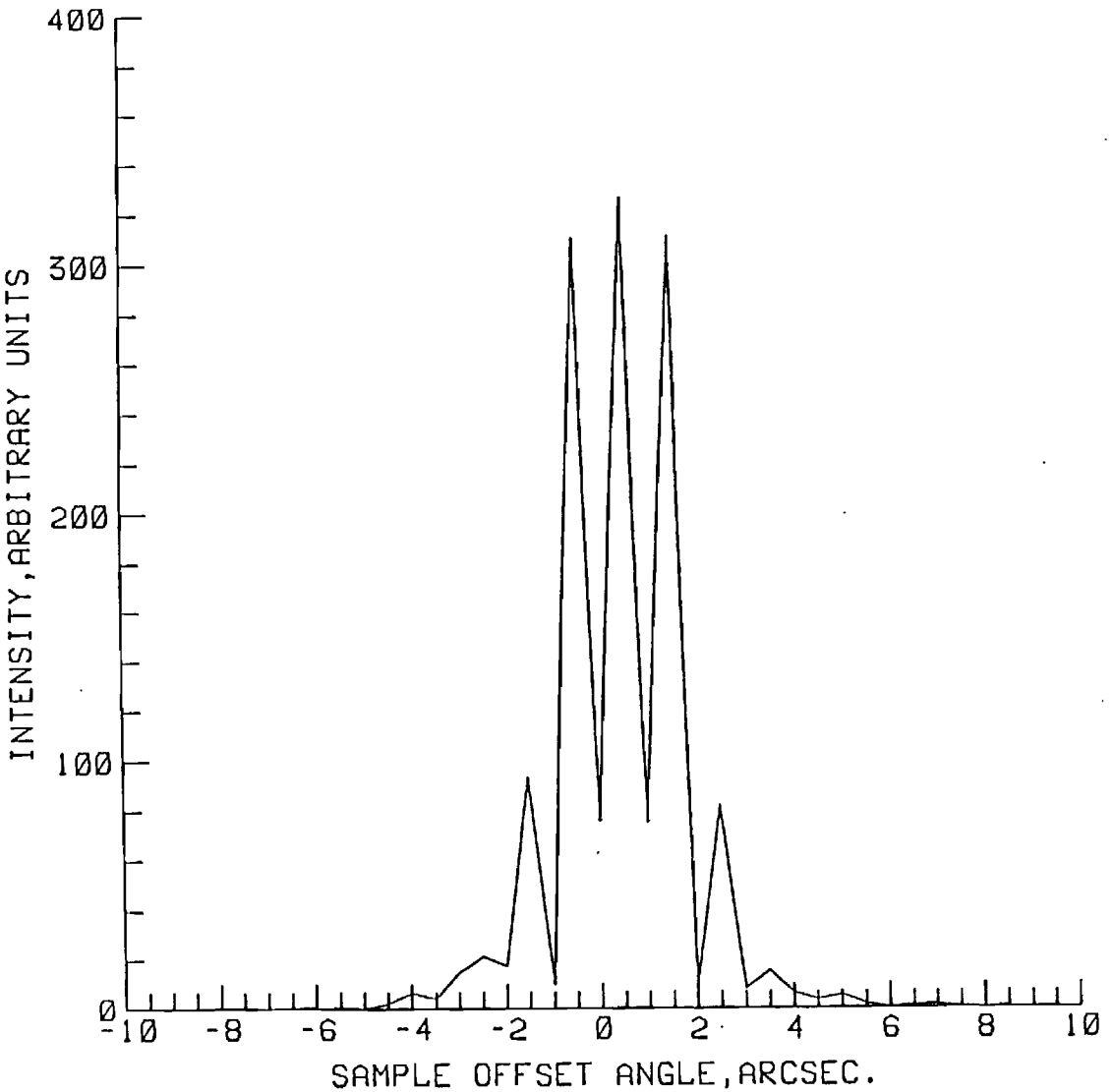
400
300
200
100
0
INTENSITY, ARBITRARY UNITS
-10
-8
-6
-4
-2
0
2
4
6
8
10
SAMPLE OFFSET ANGLE, ARCSEC.

Fig. 2b

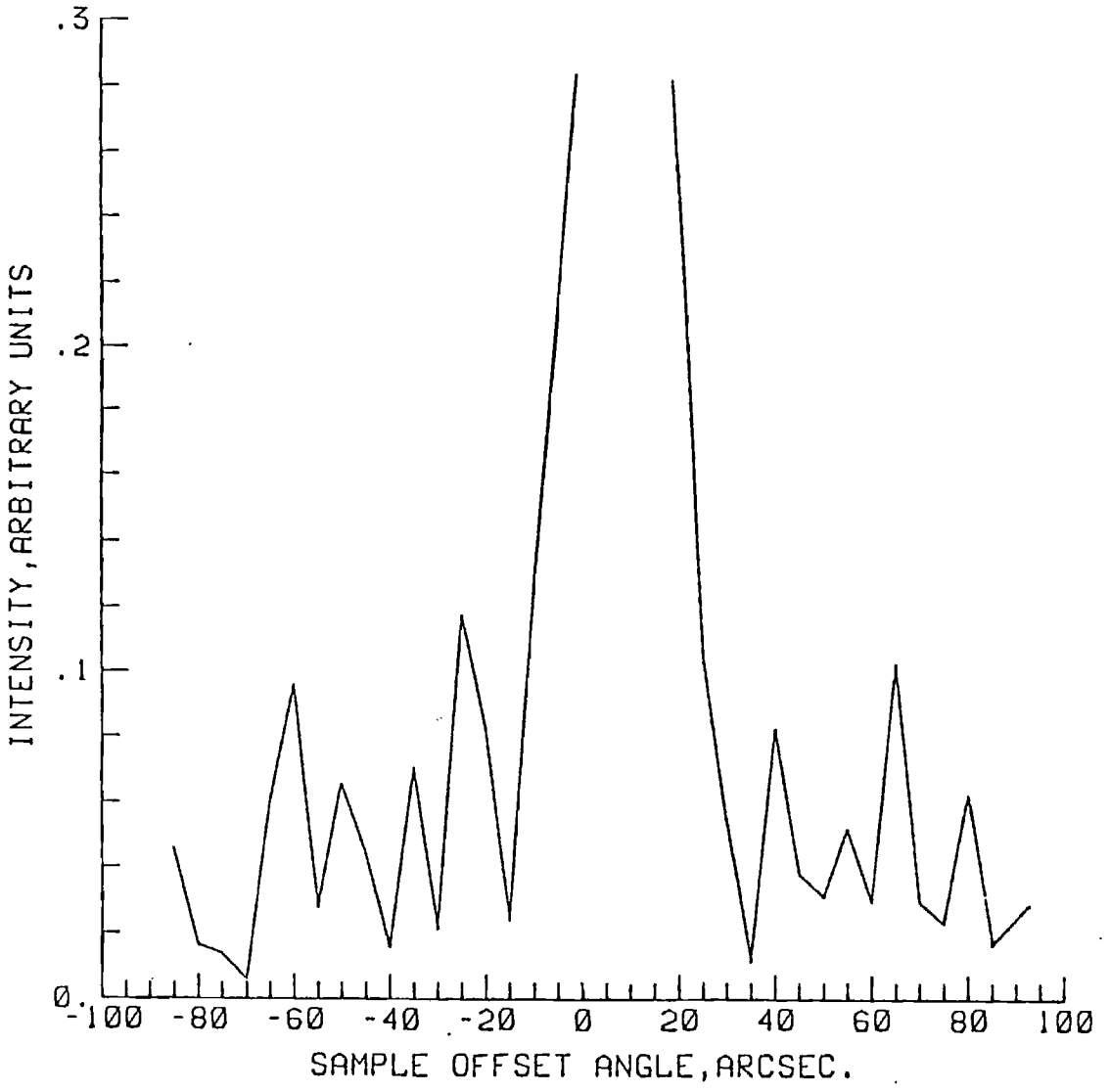
.3
.2
.1
0.
INTENSITY, ARBITRARY UNITS
-100
-80
-60
-40
-20
0
20
40
60
80
100
SAMPLE OFFSET ANGLE, ARCSEC.

Fig. 2c

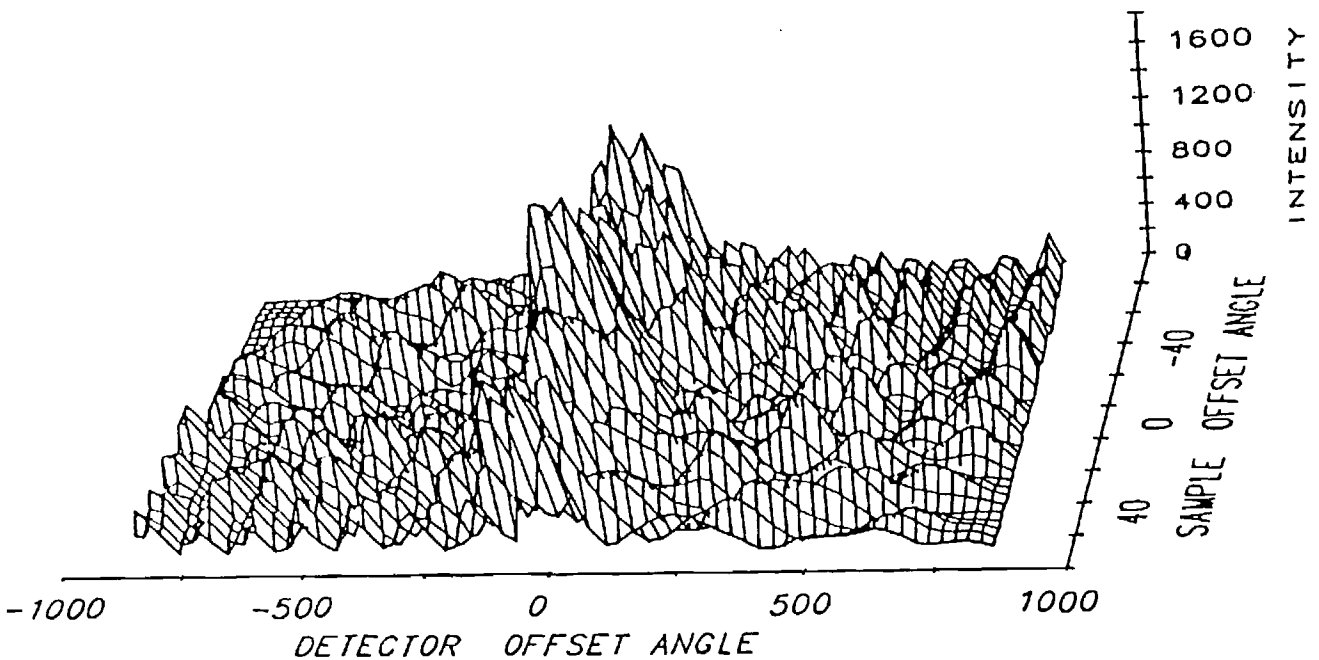
1600
1200
800
400
0
INTENSITY
40
0
-40
SAMPLE OFFSET ANGLE
-1000
-500
0
500
1000
DETECTOR OFFSET ANGLE

Fig. 3a

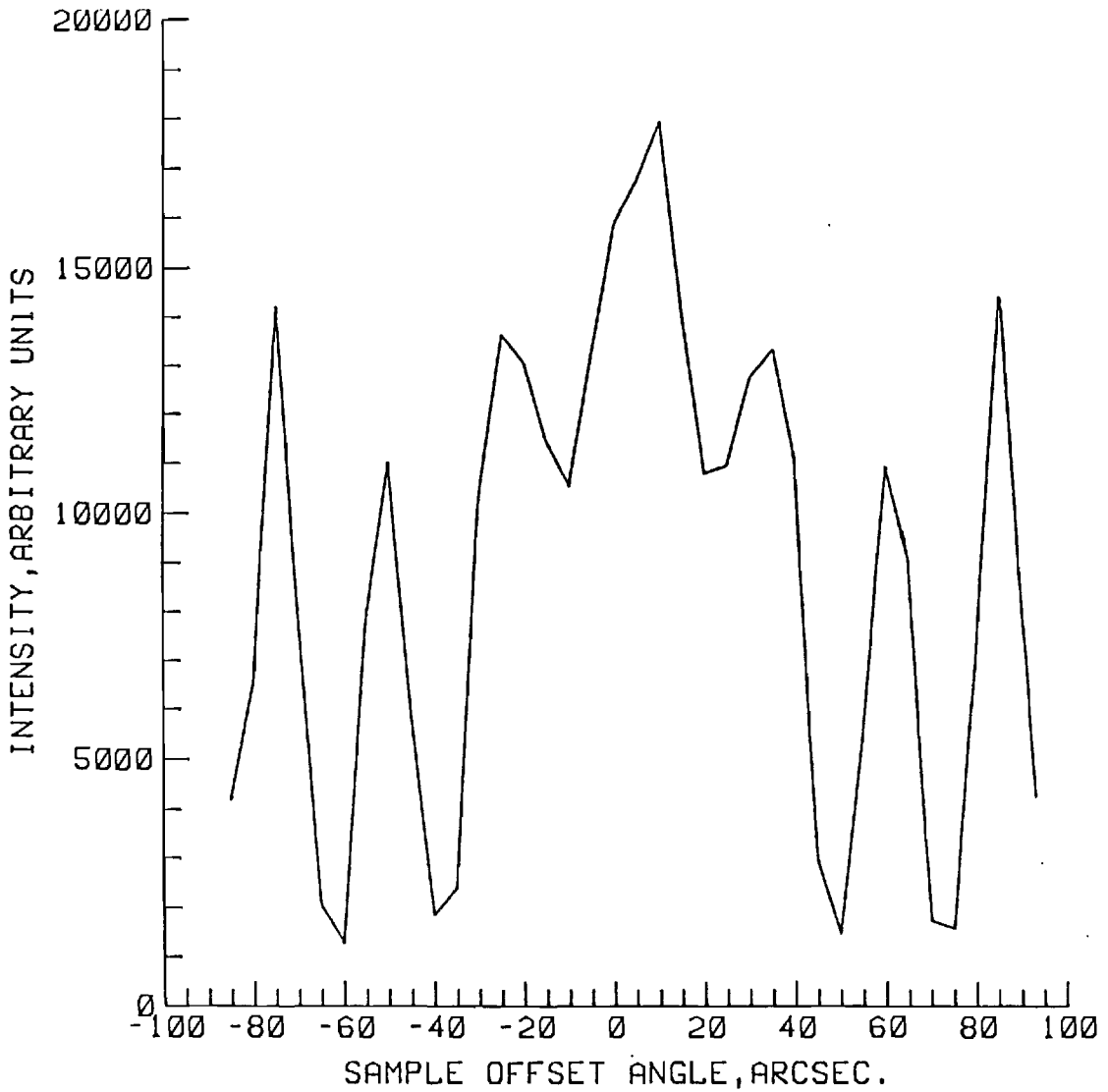
20000
15000
10000
5000
0
INTENSITY, ARBITRARY UNITS
-100 -80 -60 -40 -20 0 20 40 60 80 100
SAMPLE OFFSET ANGLE, ARCSEC.